Research article JHEP|Reports

Imaging and immunometabolic phenotyping uncover changes in the hepatic immune response in the early phases of NAFLD

Authors

Ariane Barros Diniz, Maísa Mota Antunes, Viviane Aparecida de Souza Lacerda, … André Gustavo Oliveira, Rafael Machado Rezende, Gustavo Batista Menezes

Correspondence

menezesgb@ufmg.br (G.B. Menezes).

Graphical abstract

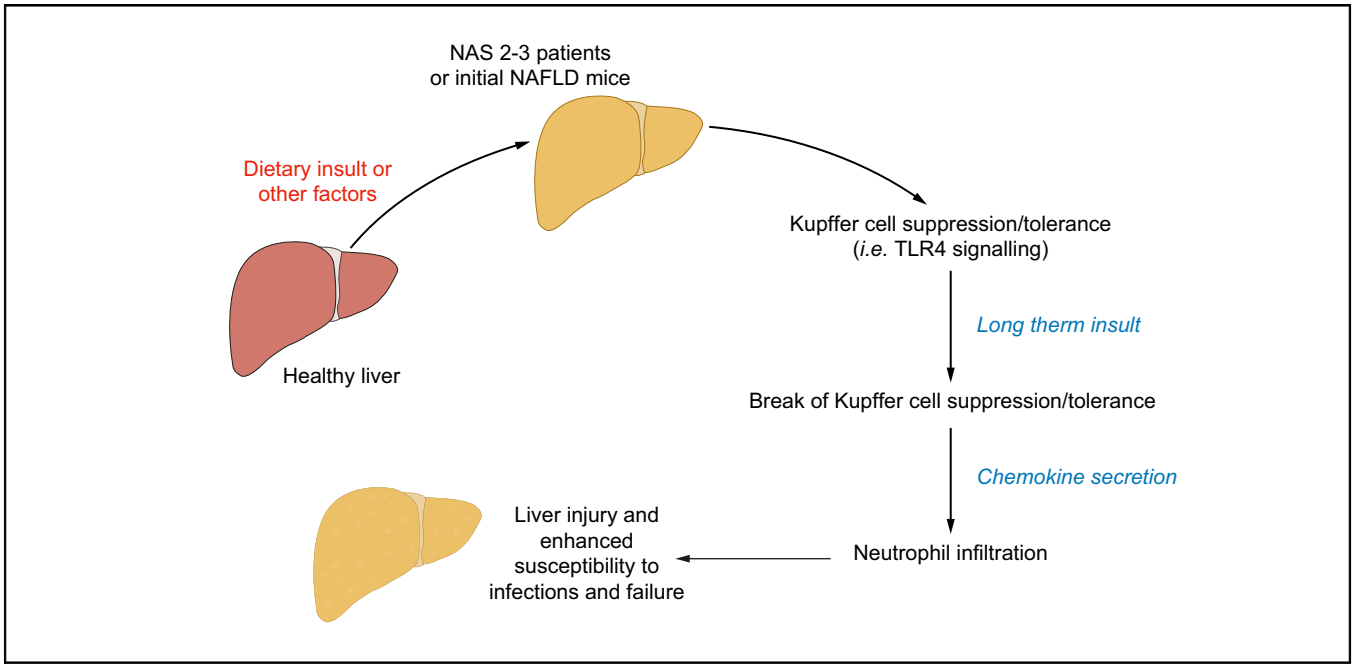

Highlights

- Hepatic immune response is already altered in liver biopsies from patients with mild NAFLD.
- We designed a novel mouse model to mimic mild NAFLD, enabling the chronological mapping of liver changes.
- This revealed an increased mortality rate upon secondary liver damage and a window of increased susceptibility to infection.
- NAFLD diagnosis may be significantly improved by a more profound investigation of changes in hepatic immunology.
- These data could guide customized nutritional and therapeutic interventions at different stages of NAFLD.

Lay summary

Fatty liver is a very common form of hepatic disease, leading to millions of cases of cirrhosis every year. Patients are often asymptomatic until becoming very sick. Therefore, it is important that we expand our knowledge of the early stages of disease pathogenesis, to enable early diagnosis. Herein, we show that even in the early stages of fatty liver disease, there are significant alterations in genes involved in the inflammatory response, suggesting that the hepatic immune system is disturbed even following minor and undetectable changes in liver fat content. This could have implications for the diagnosis and clinical management of fatty liver disease.

https://doi.org/10.1016/j.jhepr.2020.100117

Research article

JHEP|Reports

Imaging and immunometabolic phenotyping uncover changes in the hepatic immune response in the early phases of NAFLD

Ariane Barros Diniz,[1] Maísa Mota Antunes,[1] Viviane Aparecida de Souza Lacerda,[1] Brenda Naemi Nakagaki,[1] Maria Alice Freitas Lopes,[1] Hortência Maciel de Castro-Oliveira,[1] Matheus Silvério Mattos,[1] Kassiana Mafra,[1] Camila Dutra Moreira de Miranda,[1] Karen Marques de Oliveira Costa,[1] Mateus Eustáquio Lopes,[1] Débora Moreira Alvarenga,[1] Raquel Carvalho-Gontijo,[2] Sarah Cozzer Marchesi,[1] Debora Romualdo Lacerda,[3] Alan Moreira de Araújo,[4] Érika de Carvalho,[1] Bruna Araújo David,[5] Mônica Morais Santos,[6] Cristiano Xavier Lima,[3] Juliana Assis Silva Gomes,[3] Tereza Cristina Minto Fontes Cal,[3] Bruna Roque de Souza,[3] Cláudia Alves Couto,[3] Luciana Costa Faria,[3] Paula Vieira Teixeira Vidigal,[3] Adaliene Versiane Matos Ferreira,[3] Sridhar Radhakrishnnan,[7] Matthew Ricci,[7] André Gustavo Oliveira,[3] Rafael Machado Rezende,[8] Gustavo Batista Menezes[1,*]

[1]*Center for Gastrointestinal Biology, Departamento de Morfologia, Instituto de Ciências Biológicas, Universidade Federal de Minas Gerais, Belo Horizonte, Minas Gerais, 31270-901, Brazil;* [2]*Department of Molecular Medicine, The Scripps Research Institute, La Jolla, CA, Monica, USA;* [3]*Universidade Federal de Minas Gerais, Belo Horizonte, Minas Gerais, 31270-901, Brazil;* [4]*Department of Pharmacodynamics, University of Florida, College of Pharmacy, Gainesville, FL, USA;* [5]*University of Calgary, Alberta, T2N 4N1, Canada;* [6]*Laboratório de Morfologia, Departamento de Biologia Animal, Universidade Federal de Viçosa, Viçosa, Brazil;* [7]*Research Diet, Inc., New Brunswick, USA;* [8]*Ann Romney Center for Neurologic Diseases, Brigham and Women's Hospital, Harvard Medical School, Boston, MA, USA*

JHEP Reports **2020.** https://doi.org/10.1016/j.jhepr.2020.100117

Background & Aims: The precise determination of non-alcoholic fatty liver disease (NAFLD) onset is challenging. Thus, the initial hepatic responses to fat accumulation, which may be fundamental to our understanding of NAFLD evolution and clinical outcomes, are largely unknown. Herein, we chronologically mapped the immunologic and metabolic changes in the liver during the early stages of fatty liver disease in mice and compared this with human NAFLD samples.

Methods: Liver biopsies from patients with NAFLD (NAFLD activity score [NAS] 2–3) were collected for gene expression profiling. Mice received a high-fat diet for short periods to mimic initial steatosis and the hepatic immune response was investigated using a combination of confocal intravital imaging, gene expression, cell isolation, flow cytometry and bone marrow transplantation assays.

Results: We observed major immunologic changes in patients with NAS 2–3 and in mice in the initial stages of NAFLD. In mice, these changes significantly increased mortality rates upon drug-induced liver injury, as well as predisposing mice to bacterial infections. Moreover, deletion of Toll-like receptor 4 in liver cells dampened tolerogenesis, particularly in Kupffer cells, in the initial stages of dietary insult.

Conclusion: The hepatic immune system acts as a sentinel for early and minor changes in hepatic lipid content, mounting a biphasic response upon dietary insult. Priming of liver immune cells by gut-derived Toll-like receptor 4 ligands plays an important role in liver tolerance in initial phases, but continuous exposure to insults may lead to damage and reduced ability to control infections.

Introduction

Non-alcoholic fatty liver disease (NAFLD) is currently the most common form of chronic disorder, affecting more than a quarter of the world's population.[1,2] Recent studies have predicted that the number of patients with NAFLD is expected to double or triple over the next 10 years, becoming the leading cause of liver transplantation.[3–5] NAFLD can be considered as the hepatic expression of the metabolic syndrome, while associated risk factors, including obesity, insulin resistance and type 2 diabetes, can fuel the progression of NAFLD.[6,7] It is even more concerning that at least 10% of children are already developing steatosis[1]; therefore, in addition to educational actions directed to appropriate nutrition, expanding our knowledge on the pathogenesis of NAFLD – mainly in the initial stages - is of great interest.

It is well accepted that the gold standard for diagnosing NAFLD remains a liver biopsy. Despite the advances in technologies that track molecular markers in the blood or high-end imaging approaches, NAFLD detection in the general

Keywords: NAFLD; liver; steatosis; immune system; diet; metabolism; *in vivo* imaging; immunity.

Received 9 January 2020; received in revised form 2 March 2020; accepted 26 March 2020; available online 20 April 2020

* Corresponding author. Address: Center for Gastrointestinal Biology, Departamento de Morfologia, Instituto de Ciências Biológicas, Universidade Federal de Minas Gerais, Av. Antonio Carlos, 6627 - Belo Horizonte, Minas Gerais, 31270-901, Brazil. Tel./fax: +5531 3409 3015.

E-mail address: menezesgb@ufmg.br (G.B. Menezes).

population is still challenging.[8,9] Due to this relative lack of reliable disease markers, most patients with NAFLD are considered as asymptomatic for long periods of the disease. Therefore, the precise onset of NAFLD in patients, which could provide important insights on the chronological evolution of the disease and early diagnosis markers, is still obscure. In this scenario, millions of patients develop cirrhosis before being diagnosed, with an annual economic burden estimated at €200 billion in Europe[4] and more than US$100 billion in the United States.[10]

Using mice to model the NAFLD spectrum displayed by humans may be extremely challenging. For this, long-term dietary protocols – up to 30 weeks of challenge using diets that have imbalanced micronutrient composition – are the most common choice.[11–13] However, such protocols – that induce a more severe form of NAFLD - preclude the evaluation of the initial events triggered by the diet, which may represent an important period for patients with NAFLD. Herein, we measured gene expression of different inflammatory pathways in liver biopsies from patients diagnosed with NAFLD (NAFLD activity score [NAS] 2–3). We found several alterations in genes involved in the immune response, including a high expression of Toll-like receptor 4 (*TLR4*) mRNA. Moreover, using a novel short-term scheme of dietary insult (2–9 weeks), we fully mapped NAFLD development in mice, which allowed an extensive chronological characterization of the immunologic and metabolic changes in the liver. We showed that mice in the first stages of NAFLD mounted an overt inflammatory response to a non-lethal drug-induced liver injury, leading to 100% mortality in the first 24 h. In addition, early stage NAFLD mice displayed increased susceptibility to bacterial infections, which may be explained by the profound alterations observed in both number and function of hepatic macrophages. In addition, we revealed that amongst different immunologic pathways, TLR4 signaling in liver cells might drive immune tolerance in the initial phases of NAFLD, since specific TLR4 ablation led to overt expression of several pro-inflammatory mediators in Kupffer cells and enhanced chemokine signaling in the liver upon challenge. Together, these data revealed a previously unappreciated window of susceptibility to liver damage and infection in the initial stages of NAFLD.

Materials and methods

Animals and diets

Twelve- to 14-week old male C57/BL6 wild-type (WT) and *Tlr4* knockout (*Tlr4*$^{-/-}$) mice were from Centro de Bioterismo in Universidade Federal de Minas Gerais (CEBIO – UFMG, Brazil). Mice were maintained under controlled temperature (24°C) and luminosity (light/dark cycle of 12/12 h), with chow and water *ad libitum*. Mice were fed a standard low-fat control diet (hereafter termed standard diet "SD" – D12450J – 10% of calories derived from fat) or high-fat diet (hereafter termed "HFD" – D12492 – 60% of calories derived from fat) for 2, 4, 6 or 9 weeks. Diets were supplied by Research Diets (New Jersey, USA). Diet composition can be found in Table S1. All animal studies were approved by the Animal Care and Use Committee at UFMG (CEUA 392/2016).

Body weight and adiposity index

Mice were weighed weekly throughout the experimental period and the adiposity index was calculated as in.[14]

Oral glucose tolerance test and Insulin tolerance test

For the oral glucose tolerance test, mice were fasted for 6 h and then received an oral D-glucose solution (2 g/kg per gavage). For the insulin tolerance test, mice were in a fed state and received an insulin solution (0.75 UL/kg i.p. Humulin® - Lilly). Capillary glucose and insulin tolerance tests were performed as in.[15]

Biochemical analyses

Serum alanine aminotransferase (ALT) activity was assessed as described in.[14] Adipokines, serum glucose and cholesterol, serum and liver triglycerides levels, were measured as described in.[16] Hepatic total fat content was extracted by the Folch method.

Liver function test and histopathology techniques

Indocyanine green (Sigma-Aldrich) was measured as previously described.[17] For H&E analyses, liver and epididymal adipose tissue fragments were collected. Liver frozen sections were used for Oil Red O staining as described in.[18] Human H&E slides were collected from the Instituto Alfa de Gastroenterologia do Hospital das Clínicas – UFMG. The procedures with human samples are in accordance with Registration number in Ethics in Human Research Committee (Registration number: CAAE 56184716.3.0000.5149) and informed consent was obtained from all participants.

Intravital confocal microscopy

Confocal intravital imaging was performed as described.[19] Prior to surgery, mice received a single dose or a mixture of the antibodies described in the supplementary CTAT table. To visualize the lipid droplets *in vivo*, the dye Bodipy (1.5 μg/mouse diluted in methanol) was applied directly to the liver after surgery. F4/80+ cells were considered as Kupffer cells, and due to phenotyping limitations, some of these cells might also comprise F4/80+ infiltrating monocytes.[20] Images were obtained using Nikon Eclipse Ti with an A1R confocal (Nikon Instruments Inc., USA).

Primary murine hepatocytes and liver non-parenchymal cells

Primary hepatocyte purification was performed as described previously.[21] Liver non-parenchymal cells (LNPCs) from mice were isolated as reported previously.[17] For flow cytometry, cells were stained with antibodies described in the supplementary CTAT table. Events were acquired using Accuri C6 Flow cytometer (BD biosciences, USA) and analyzed using FlowJo (FlowJo, USA). In a separate set of experiments, Kupffer cells were sorted as F4/80^{+} cells using magnetic beads.[22]

Systemic *E. coli* injection and colony forming unit determination

Analysis of systemic bacterial infection (assessed by colony forming units [CFUs] and bacterial clearance *in vivo*) and flow cytometry were performed as described in.[17] For *in vivo* imaging of *Escherichia coli* (*E. coli*) capture, mice received 5 × 10^{7} GFP-expressing *E. coli* intravenously, and were imaged under confocal microscopy for 10 min.

Drug-induced liver injury model

Mice were fasted for 12–15 h before acetaminophen (APAP) (400 mg/kg) or vehicle administration.[14,23,24] APAP (Sigma-Aldrich, St. Louis, MO, USA) was dissolved in a warm 0.9% saline solution at a concentration of 50 mg/ml prior to gavage.

Gene expression by real-time PCR

Total RNA samples were isolated from total liver, hepatocytes, LNPCs and Kupffer cells from mice and from the livers of human biopsies (Registration number in Ethics in Human Research Committee: CAAE 67583317.3.0000.5149). Patients with NAFLD involved in this study were diagnosed using liver biopsies, and only patients with NAS 2–3[25] were included. NAFLD was considered after exclusion of other liver diseases. Samples from healthy patients were collected from livers that were selected for donation (Table S3). Absence of liver diseases was confirmed from medical records and histopathology. Informed consent was obtained from all participants, Real-time PCR was performed as described in.[17] A list of primers sequences can be found in the supplementary CTAT table.

Bone marrow chimera generation

Bone marrow chimeras were generated as described.[14] Irradiated recipients (WT or *Tlr4*$^{-/-}$) received 1 × 10^7 bone marrow cells from either WT or *Tlr4*$^{-/-}$ mice intravenously. Mice had a recovery period of 8 weeks before experiments.

Statistical analysis

Experimental data were analyzed using one-way ANOVA with Tukey's *post hoc* test and unpaired Student's *t* test provided by Prism 6.0 software (GraphPad). All data are given as the mean ± SEM. Differences were considered significant at $p < 0.05$.

Results

Immunologic alterations in liver microenvironment are already detectable in patients with NAFLD

NAFLD is characterized by varying levels of triglyceride accumulation within cytoplasmic vesicles of hepatocytes; regular histopathology and routine exams describe this condition as absent of inflammation. However, considering the large immune cell population that inhabits the liver, we hypothesize that even minor changes in hepatic microenvironment would be sensed by the resident immune system. To search for putative alterations in the expression of inflammatory genes in early phases of NAFLD, we first selected target pathways previously described as relevant in the context of hepatic inflammatory responses, and measured their expression in liver biopsies from patients that were diagnosed with a mild grade of steatosis based on a NAS of 2 or 3[25] (Fig. 1A). Patients included in this analysis had normal or minor alterations in clinical levels of liver aminotransferases in serum, had no other metabolic diseases (including type 2 diabetes) and were classified as obese or overweight (Table S2). Real-time PCR analysis revealed that patients with NAS 2–3 already presented alterations in the expression of different inflammatory genes. We observed a significant downregulation of interleukin 1 beta (*IL1B*) and transforming growth factor beta 1 (*TGFB1*) mRNA expression, which was accompanied by a concomitant and massive upregulation of *TLR4* expression (Fig. 1B). Analysis of other relevant immune-related genes, including *IL10, TNF, IL6, IFNG, VEGF* and *TLR2* revealed no significant alterations. Thus, this suggests that changes in the hepatic immunologic response in specific inflammatory genes might be an important event in patients with NAS 2–3. Importantly, these alterations in inflammatory gene expression may be used as an additional tool for NAFLD diagnosis in early stages.

Short-term ingestion of HFD leads to subclinical body changes, but drives massive lipid accumulation within the liver

The precise determination of NAFLD onset in patients is extremely challenging, and the relative lack of a chronological understanding in disease evolution is a major issue in NAFLD research. To mimic the mild grades of NAFLD in humans, and perform a controlled chronological investigation of NAFLD establishment, we developed a protocol using a short-term dietary challenge in mice. Our experimental scheme is presented in Fig. 2A. To assure that all mice were age-matched at the sample collecting time point, we started the dietary challenge at different ages. Of note, mice fed SD during all time points had no detectable changes in all parameters analyzed in this study; thus, they were grouped as "SD" from here on. As shown in Fig. 2, mice fed an HFD had no detectable weight gain over the experimental period (Fig. 2B). Although we observed a significant change in body fat composition (adiposity index), liver/body weight ratio was not altered throughout the dietary challenge. In addition, no significant alterations in serum or hepatic levels of triglycerides, or in serum levels of free fatty acids were observed (Fig. 2H–J and Fig. S1E). Mice evolved to hyperglycemia only after 4 and 9 weeks of HFD, which may reflect an increased glucose intolerance and resistance to insulin (Fig. 2H–J and Fig. S1C,D). In this scenario, increased levels of serum cholesterol were the only clinical alteration detected in the 2nd week post challenge (Fig. 2G). Despite no weight gain during HFD challenge, mice displayed a progressive increase in body adiposity at later time points, starting at the 6th week post challenge (Fig. 2C). Histological analysis of epididymal adipose tissue revealed that along with a significant increase in body adiposity index, the average area of adipocytes was significantly larger than in controls after 4 weeks of the HFD protocol – this was sustained up to the 9th week (Fig. 2K and L). Despite these histological changes, crown-like structures – a sign of immune cell infiltration – were not observed. Interestingly, serum levels of adiponectin, a clinical marker that can be used to predict the severity of obesity and metabolic syndrome, were not altered in this experimental protocol (Fig. 2M). In line with this, serum ALT levels did not change during HFD ingestion, suggesting that no detectable hepatic parenchymal damage was generated. To confirm that the liver function was not altered by the HFD regimen, we directly assessed the hepatic ability to clear indocyanine green from the circulation (Fig. 2O). We found no significant differences among the analyzed groups. Together, these data indicate that despite major changes in body fat content and in glucose management, several clinical markers of systemic diseases, and particularly liver function, were not altered using a short-term HFD challenge.

To further visualize the hepatic microenvironment, we processed liver samples from different groups for histopathology. We did not find any alterations in liver histology compared to SD-fed mice in the 2nd week of challenge. At a later time point (6 weeks post HFD regimen), a discrete macrovesicular pattern in the centrilobular region (black arrows), suggestive of initial steatosis, was detected (Fig. 2N). However, histologic features of NAFLD including general steatosis, ballooning, and lobular inflammation (black arrows) were only found in mice fed HFD for 9 weeks (Fig. 2N). To image lipid accumulation at a higher definition and under physiological conditions, we developed a novel methodology to stain and quantify lipid droplets *in vivo*,

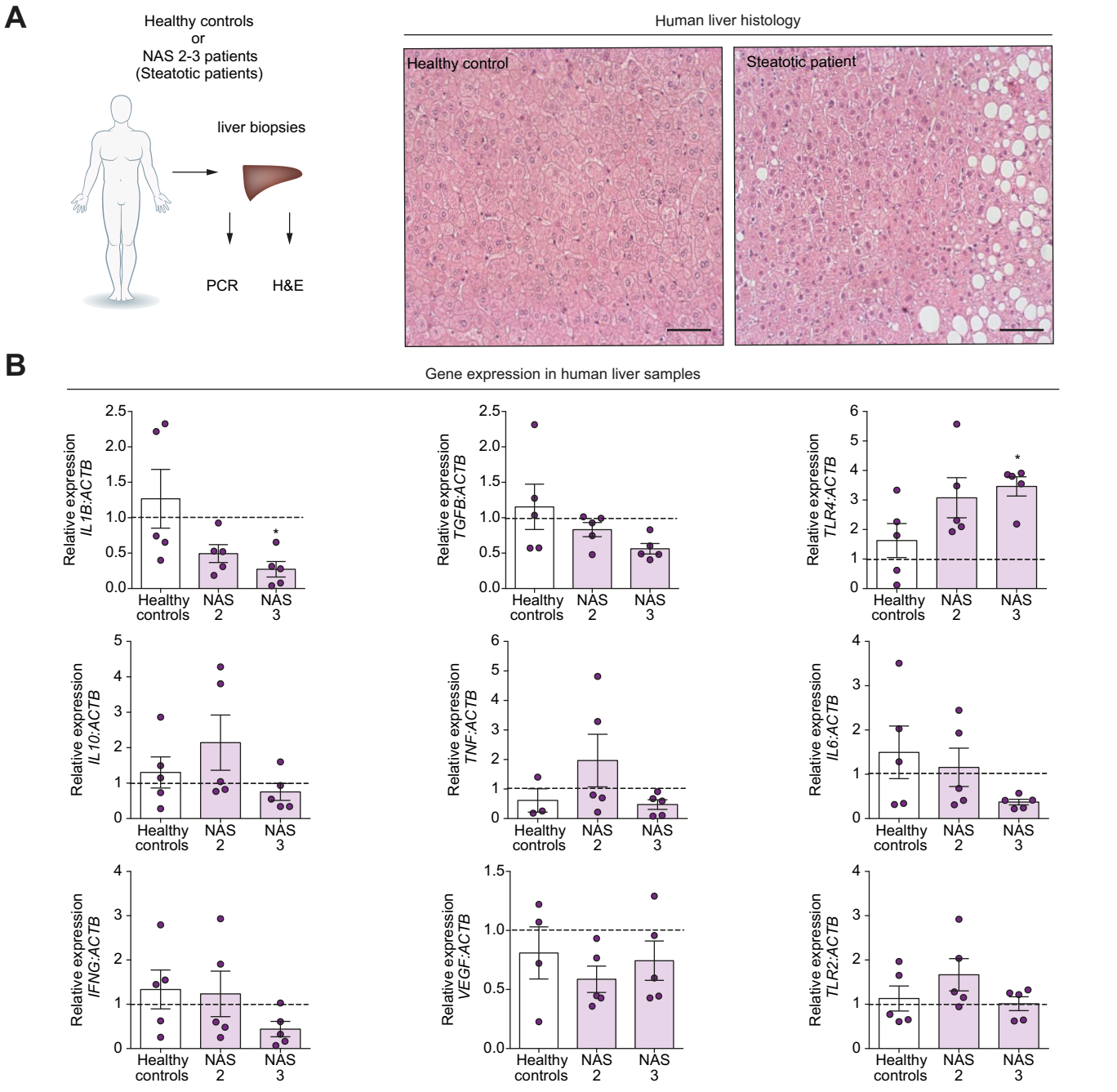

Fig. 1. Expression of inflammation-related genes in human liver biopsies. Expression of different immune system-related genes in samples from patients with NAS 2–3 and healthy controls. (A) Histopathology selected from a healthy donor (normal findings) and NAS 2 patient showing initial steatosis. All biopsies were analyzed by an experienced pathologist prior to gene expression assays. (B) Gene expression assessed by Real-Time PCR. Fold change was normalized by values found in healthy control samples. Bar = 50 μm. *p <0.05 compared to healthy controls. One-way ANOVA. NAFLD, non-alcoholic fatty liver disease; NAS, NAFLD activity score.

allowing the visualization of the hepatic microenvironment under confocal intravital microscopy (Fig. 3). We found that the HFD-challenged group displayed a progressive accumulation of lipid droplets within the liver, which could now be detected, and was significantly enhanced as early as 2 weeks post challenge (Fig. 3A–D). Interestingly, while classic Oil red O staining confirmed the validity of our *in vivo* fat visualization protocol (Fig. S1A), regular H&E staining failed to detect such alterations. In fact, we observed a linear trend of intensification in the number, frequency and area of lipid droplets throughout the HFD challenge (Fig. 3B–D). To map the precise sites of lipid accumulation within the liver compartments, we stained both liver sinusoids and lipid droplets, and rendered three-dimensional reconstructions using intravital microscopy (Fig. 3E). We found that lipid droplets started to accumulate after 2 weeks of the HFD protocol in specific regions across the liver, but at all time points analyzed, they were mostly found in the inter-sinusoidal space, confirming their location inside hepatocytes. Taken together,

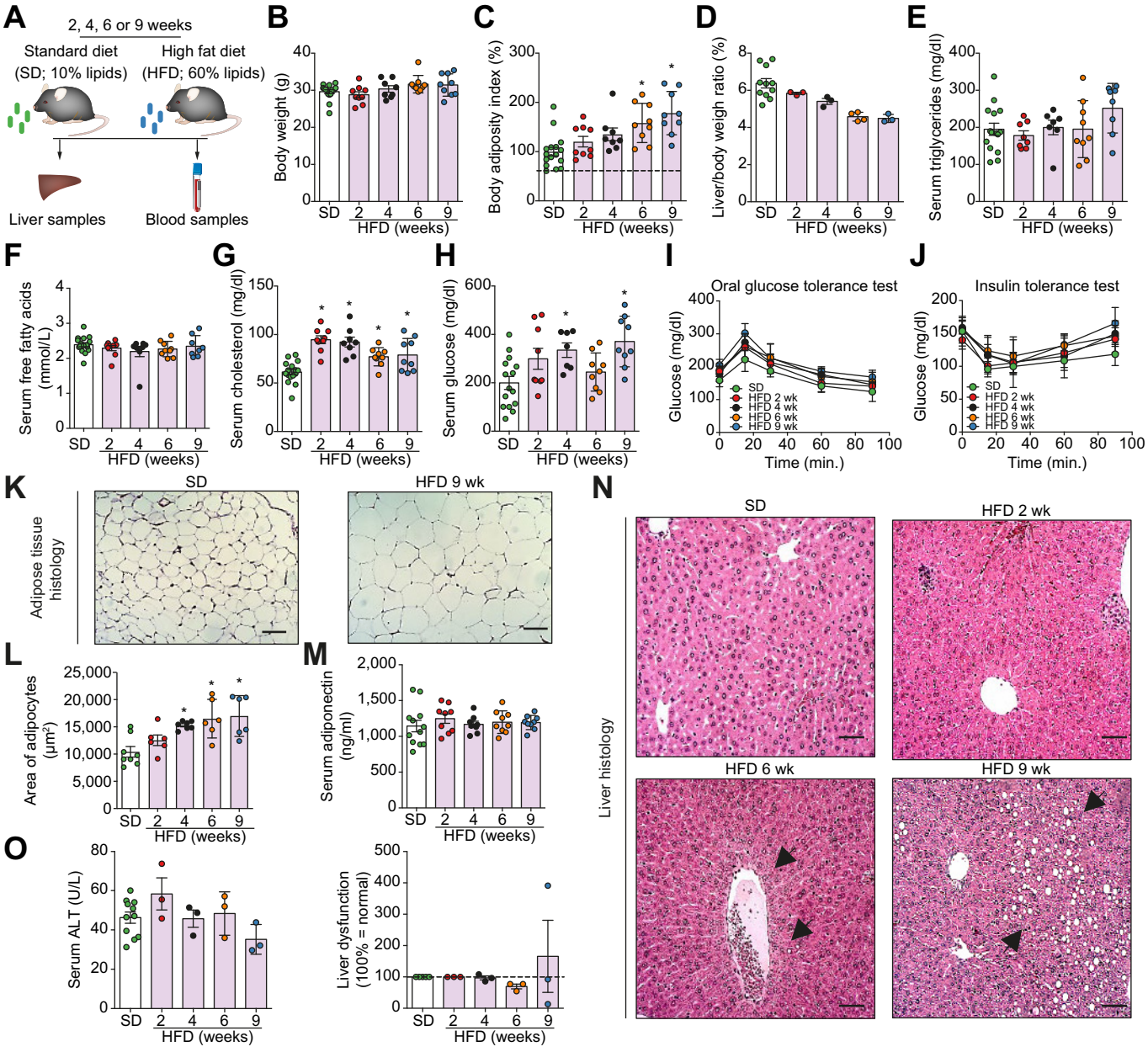

Fig. 2. Establishment of a model with subclinical body changes induced by short-term dietary insult. (A) Experimental protocol of short-term HFD. (B) Body weight of mice throughout experimental period. (C) Changes in body adiposity index during dietary challenge. (D) Liver / body weight ratio in all time points studied. (E–H) Serum levels of different clinical read-outs. (I–J) Assessment of glucose tolerance and insulin resistance in different groups. (K–L) Histologic and digital quantification of epididymal adipose tissue morphology. (M) Serum levels of adiponectin. (N–O) Liver histology, serum ALT levels and assessment of liver function using indocyanine green depuration rate. *P <0.05 compared to SD group. One-way ANOVA. Bar = 50 μm in K and N. ALT, alanine aminotransferase; HFD, high-fat diet; SD, standard diet.

these data suggest that despite minor alterations in liver histology in the initial phases of dietary challenge (2–6 weeks post HFD), lipid accumulation within the liver occurs at earlier time points, which could be more precisely detected and measured using our *in vivo* imaging protocol.

Liver immunologic environment is dramatically changed during the initial phases of high-fat challenge

There is a growing body of evidence that the liver is a central organ in immune surveillance, which is inhabited by a large and complex population of immune cells even under physiological situations.[26] However, these cells can rapidly change their proportion and phenotype following insults, and this may be associated with enhanced inflammation and liver damage. To investigate putative changes in the hepatic immune environment during the HFD protocol, we collected liver samples and isolated non-parenchymal cells for immunophenotyping using flow cytometry (Fig. 4A). We found that mice fed HFD for 2 weeks had a significant increase (~50%) in the number of T cells compared to SD-fed mice, which was not sustained at later time

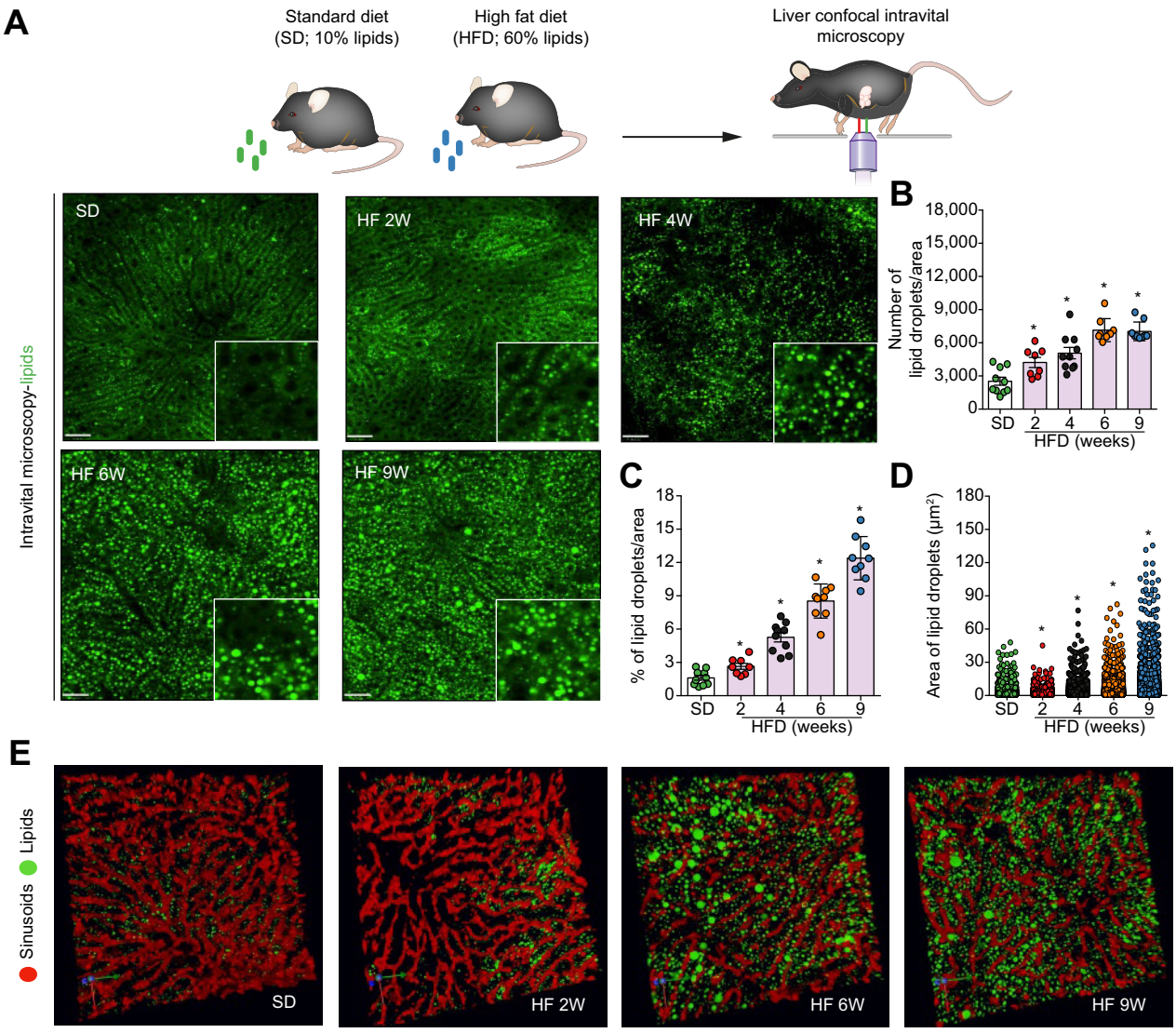

Fig. 3. Early stages of steatosis in mice visualized *in vivo* using a novel approach on confocal intravital microscopy. (A) Intravital microscopy assessment of lipid droplet deposition stained *in situ* by Bodipy. (B–D) Digital quantification *in vivo* of number, frequency and area of lipids droplets. (E) Three-dimensional reconstruction of hepatic sinusoids (anti-CD31 – in red) and lipids droplets (bodipy – in green) *in vivo*. **p* <0.05 compared to SD group. One-way ANOVA. Bar = 28 μm in A (zoom 4× in insert). HFD, high-fat diet; SD, standard diet.

points, along with a 50% reduction in dendritic cell (DC) frequency. Despite a rapid recovery after 4 weeks of HFD regimen, DC populations were significantly depleted and this was maintained until the end of the experimental protocol (9 weeks) (Fig. 4B, F). In line with this, mice sustained a significant reduction in the frequency of Kupffer cells (KCs), again with a nearly 50% reduction 6 to 9 weeks post challenge (Fig. 4G). Moreover, although unaltered following up to 6 weeks of HFD ingestion, we observed an abrupt and massive liver infiltration of neutrophils 9 weeks post challenge (~4-fold increase), constituting the most frequent immune cells within the liver at this time point (Fig. 4H).

To investigate how HFD could alter hepatic immunometabolic profile, we next isolated both LNPCs and hepatocytes to assess gene expression. We found that LNPCs from mice under HFD regimen displayed a massive suppression in genes belonging to immune response 2 weeks post challenge, including *Tnf, Il10 and Cxcl2*. Genes involved in bacterial arrest were also significantly reduced at this time point, including *Marco* and *Nr1h3* (Fig. 4I). However, LNPCs had a progressive increase in expression of almost all genes evaluated throughout the HFD protocol, which peaked for most genes in the 4th week after HFD implementation. Interestingly, *Tlr4, Marco*, *Cd163* and *Itgam* – all genes belonging to pathways related to pathogen recognition – were enhanced only at later time points following the HFD protocol. Thus, we observed a dynamic alteration pattern in the hepatic immune compartment during all periods of HFD ingestion (Fig. 4I). We also assessed gene expression in isolated hepatocytes during the HFD protocol (Fig. S2). For this, we selected different pathways belonging to P450 cytochrome, xenobiotic management and inflammatory response. Despite punctual reduction in albumin synthesis (*Alb*), glutathione transferases P1 (*Gsp1*) and *Il1b* expression, most pathways analyzed were not significantly altered in hepatocytes during the HFD experimental

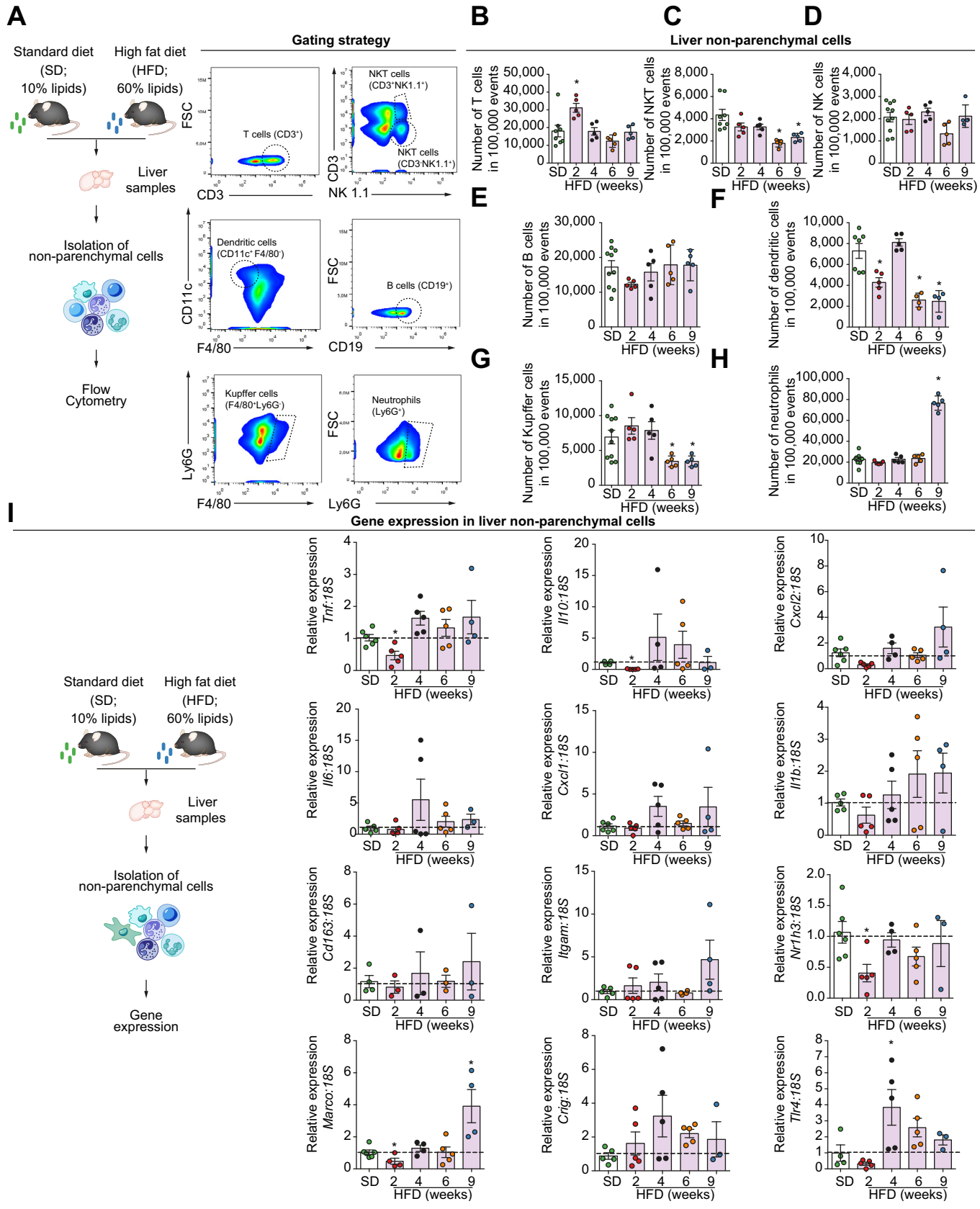

Fig. 4. Immunophenotyping by flow cytometry and gene expression in isolated liver non-parenchymal cells in initial phases of NAFLD. (A) Flow cytometry gating strategy to immunophenotype liver non-parenchymal cells. (B–H) Number of different liver leukocytes during HFD protocol compared to controls (SD). (I) Liver non-parenchymal cells were purified and gene expression was assessed by Real-Time PCR, and fold change was measured in comparison to SD. *p <0.05 compared to SD group. One-way ANOVA. HFD, high-fat diet; NAFLD, non-alcoholic fatty liver disease; SD, standard diet.

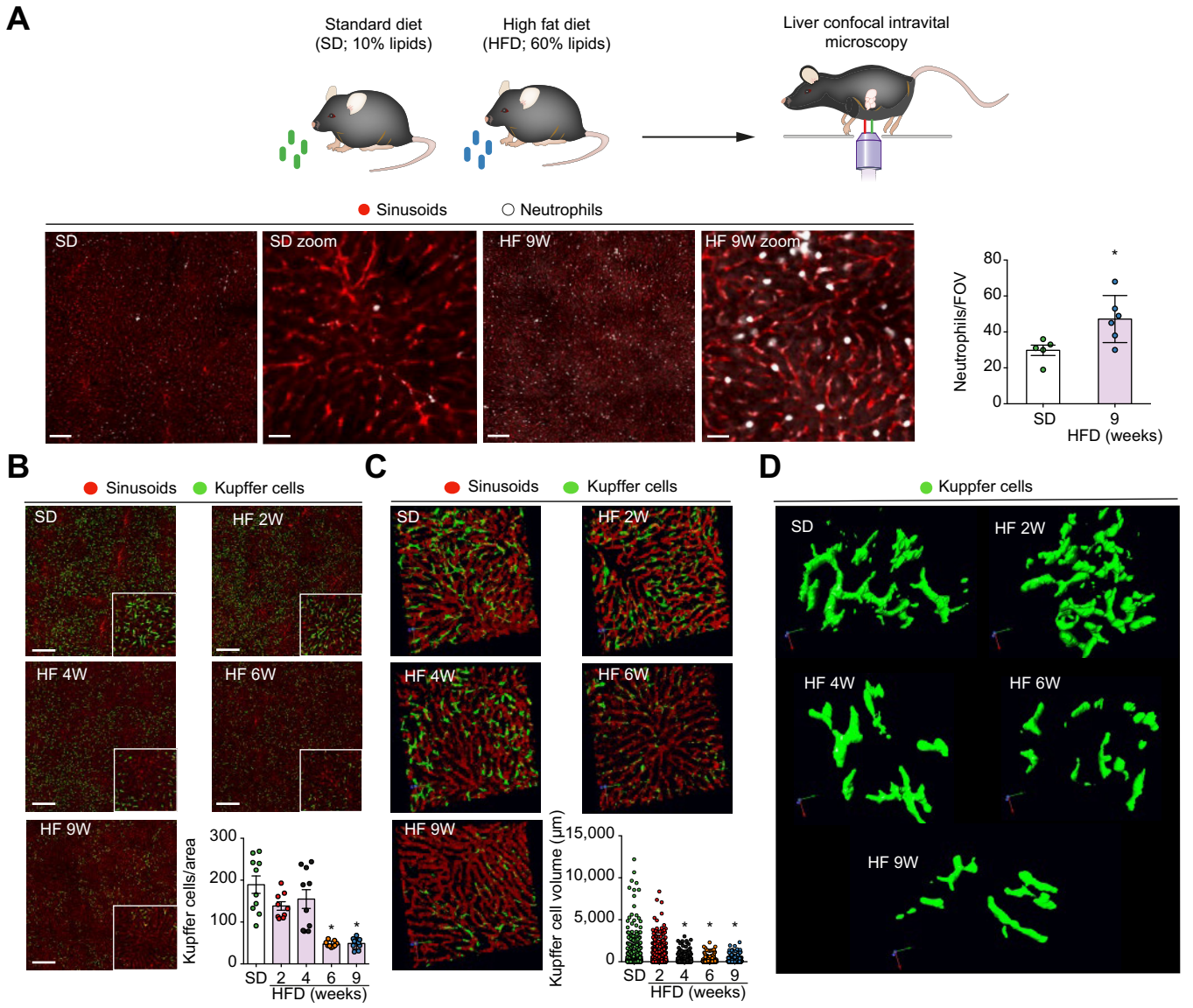

Fig. 5. Liver immune cells visualized *in vivo* in early phases of steatosis. (A) Liver intravital confocal microscopy showing accumulation of neutrophils ($Ly6G^+$ cells; in white) within liver microcirculation (anti-CD31, in red). Stitched images were composed by 24 separated images and zoomed images were digitally made using a 4× magnification. (B) Same as A, but for Kupffer cells (anti-F4/80; in green). Note significant depletion in Kupffer cell density at 6 and 9 weeks after HFD implementation. Stitched images were composed by 6 separated images. (C) Three-dimensional reconstruction of Kupffer cells under intravital confocal microscopy, showing significant reduction in cell volume over HFD challenge. (D) Three-dimensional reconstruction of individual Kupffer cells showing major alterations in cell morphology due to HFD challenge. *p <0.05 compared to SD group. One-way ANOVA. Bar = 50 µm in A, and in B = 30 µm (zoom 4× in insert). HFD, high-fat diet; SD, standard diet.

protocol (Fig. S2). Also, we found a large variation in gene expression specifically at 9 weeks post challenge, suggesting that this period may constitute a transition phase between short- and long-term HFD ingestion. Therefore, short-term HFD intake leads to alterations predominantly in the liver immune cell compartment rather than in hepatocyte metabolism, suggesting that the hepatic immune response might be particularly altered in the initial phases of NAFLD.

To image hepatic immune cells in their native environment, we prepared mice for confocal intravital microscopy (Fig. 5). For this, we stained *in vivo* liver sinusoids with anti-CD31 (in red) and counterstained neutrophils (in white) using anti-Ly6G antibody (Fig. 5A). Under physiological situations, there is a minor population of resident neutrophils in the liver, and these cells slowly patrol sinusoids. Consistent with our flow cytometry data, neutrophils avidly infiltrated within the liver at later time points of HFD ingestion (9 weeks), and these cells were restricted to the intravascular compartment, suggesting that the primary site for neutrophil adhesion during the dietary insult was the luminal environment (Fig. 5A). Under the same conditions, high definition imaging of the liver vascular compartment revealed that a large population of macrophages (KCs) is specifically located inside sinusoids, covering larger areas between post sinusoidal venules (Fig. 5B, C). HFD ingestion for up to 4 weeks caused no detectable impact on KC frequency; however, we observed a significant depletion of KCs *in vivo* compared to controls

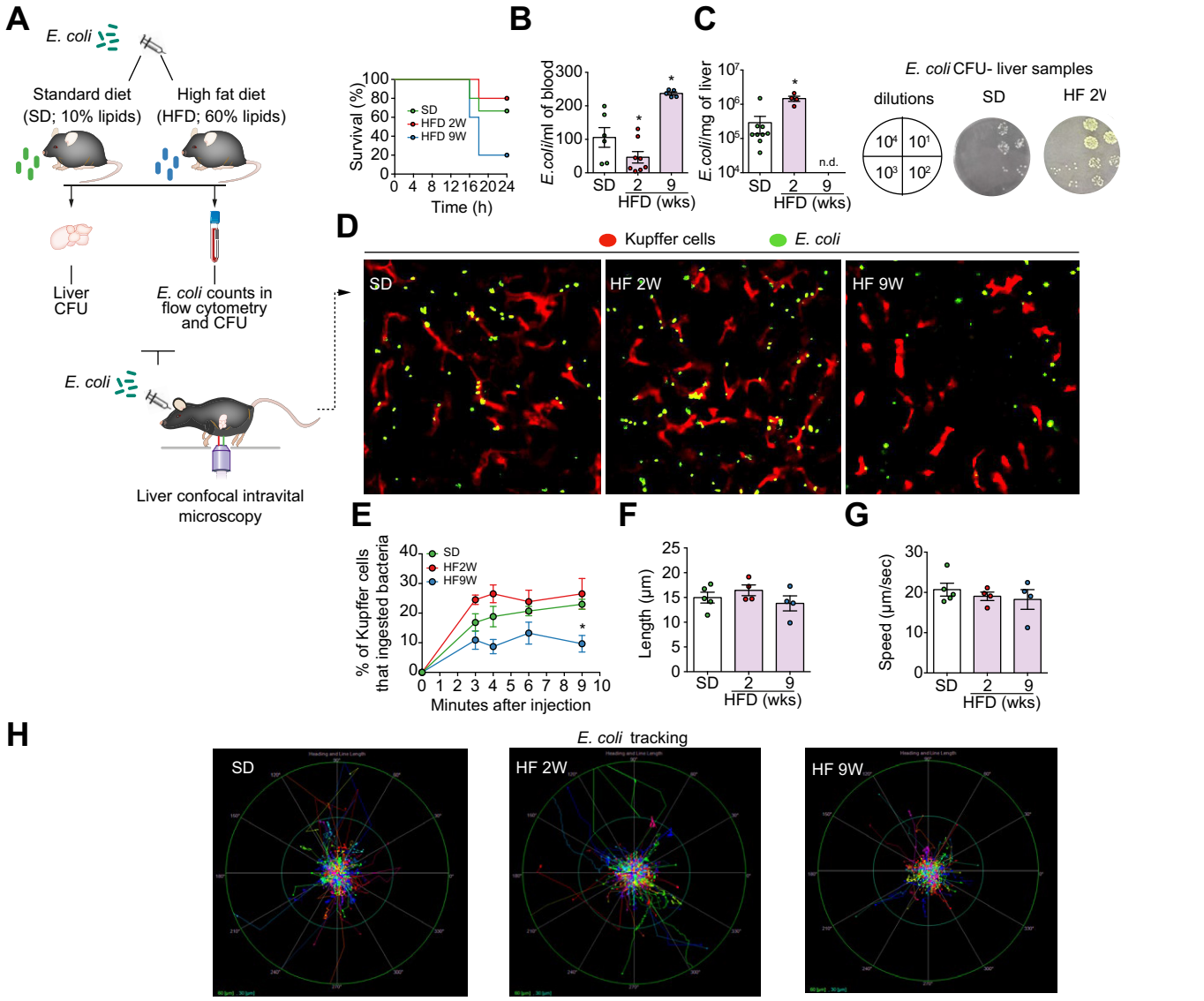

Fig. 6. Short-term dietary protocol leads to reduced ability to fight blood-borne bacterial infections. (A) Survival curve of mice during endovenous *E. coli* challenge. (B) Number of *E. coli* in circulation of mice subjected to SD or HFD protocol assessed *in vivo* by flow cytometry. (C) CFUs of *E. coli* in liver samples from mice subjected to SD or HFD protocol, along with representative images of agar plates under different dilutions. Note the significant increase of CFUs in mice challenged with HFD, and higher mortality rates in mice fed HFD 9 weeks precluded a precise determination of bacterial counts in liver samples, depicted as non-determined (n.d.). (D) Liver confocal intravital microscopy showing KCs in red (anti-F4/80) and GFP-expressing *E. coli* in green. Note that the majority of KC in SD group is engulfing bacteria, while fewer cells of HFD 9 weeks are positive for GFP. (E) Digital quantification of KC phagocytic ability. (F–H) Digital tracking of *E. coli* displacement (length) and velocity within liver sinusoids assessed by confocal intravital microscopy. *p <0.05 compared to SD group. One-way ANOVA. CFUs, colony-forming units; *E. coli, Escherichia coli*; HFD, high-fat diet; KCs, Kupffer cells; SD, standard diet.

following 6 and 9 weeks of the HFD regimen (Fig. 5B and Fig. S3A). Alterations in KC biology were not restricted to their numbers since HFD ingestion led to great changes in KC volume and morphology after as little as 4 weeks of the HFD protocol, as assessed by three-dimensional rendering of intravital microscopy and digital calculation of individual cell volume (Fig. 5C, D). In fact, KCs from HFD-challenged mice displayed fewer and smaller protrusions, which accounted for restrictions in their size and wingspan (supplementary movies 1 and 2). Considering that liver weight within the groups was not different, the significant reduction in KC frequency that we detected due to the HFD protocol was not an analysis artefact derived from liver growth (Fig. S3B), confirming that these cells are indeed depleted during liver fat accumulation.

Taking together, we showed an important shift in the hepatic immune cell environment due to short-term ingestion of a HFD, which included massive depletion of liver phagocytes (KCs and DCs), along with neutrophil infiltration within the hepatic microvasculature.

Alterations in KC number and morphology triggered in the initial phases of HFD predispose mice to infection

Pre-existing liver dysfunction is a risk factor for the progression of infection to sepsis.[27] In fact, it is becoming widely accepted

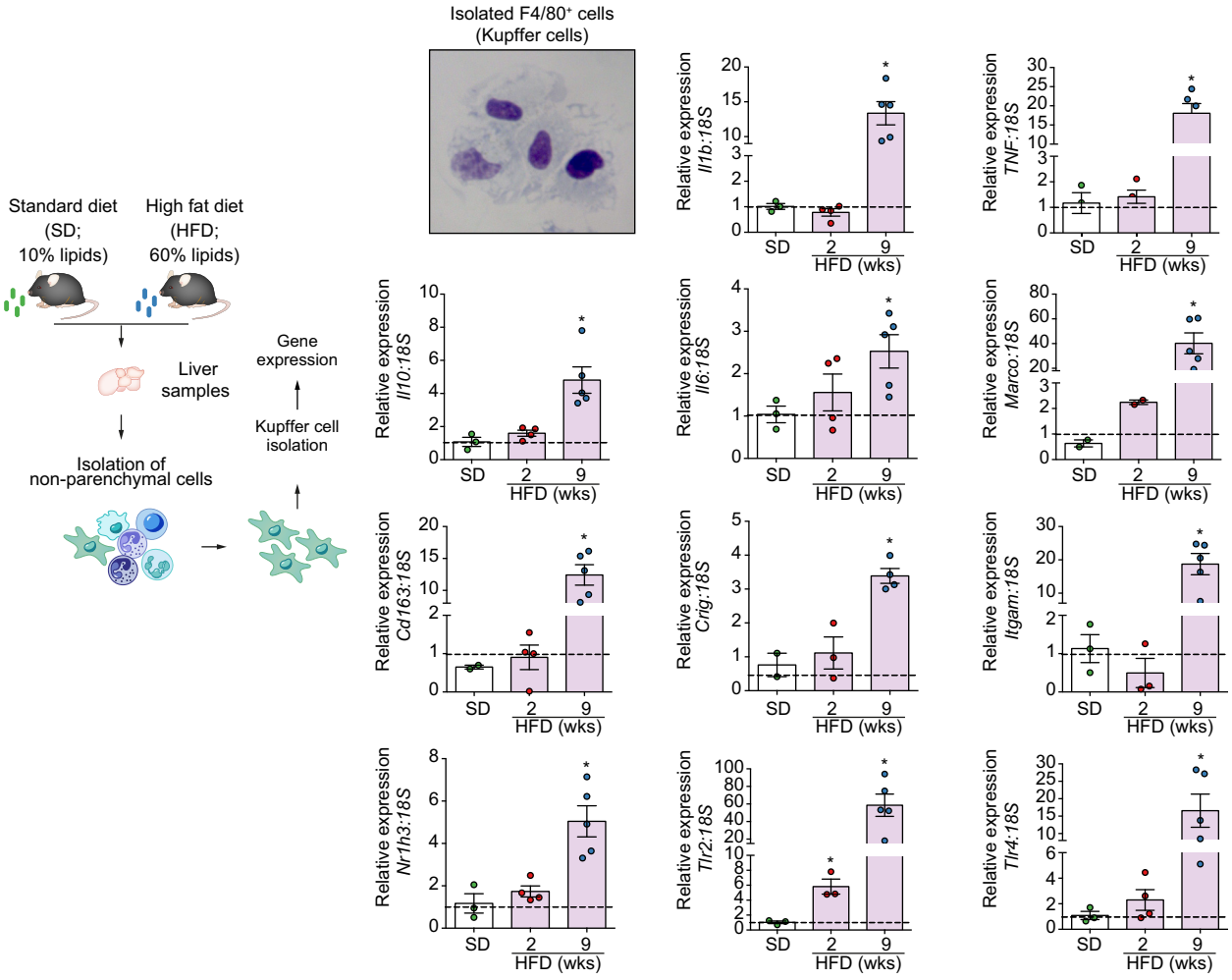

Fig. 7. Upregulation in gene expression of isolated Kupffer cells in initial phases of NAFLD. Gene expression of different immune system pathways in isolated Kupffer cells from mice fed with SD or HFD for 2 and 9 weeks. Gene expression was assessed by Real-Time PCR, and fold change was measured in comparison to SD. *p <0.05 compared to SD group. One-way ANOVA. HFD, high-fat diet; NAFLD, non-alcoholic fatty liver disease; SD, standard diet.

that the liver acts as a filter for pathogens that spread using the systemic circulation, and in this scenario, KCs are emerging as fundamental firewalls for capturing blood-borne bacteria under flow.[28,29] Based on our findings using flow cytometry and intravital imaging, we hypothesized that the changes in KC biology induced by HFD ingestion could affect the host's ability to fight infections even in the initial phases of NAFLD (Fig. 6). Thus, we challenged mice after different periods of HFD ingestion with an intravenous injection of *E. coli*. Mice fed SD and HFD for 2 weeks had ~30% and ~20% of mortality rate after infection, respectively. However, longer HFD ingestion (9 weeks) significantly increased susceptibility to infection, leading to a mortality rate of 80% after *E. coli* challenge (Fig. 6A). Despite a transient reduction in bacterial counts in the blood compared to controls, mice fed HFD for 2 weeks had a significantly higher bacterial titer in the liver (Fig. 6B, C). In line with this, longer HFD ingestion (9 weeks) led to increased bacteremia, confirming that blood clearance was significantly impaired in mice fed HFD for 9 weeks (Fig. 6B). Higher mortality rates in mice fed HFD 9 weeks precluded a precise determination of bacterial counts in liver samples (depicted as non-determined in Fig. 6C). To better understand the mechanisms underlying this susceptibility to bacterial spread observed in HFD-fed mice, we imaged phagocytosis of GFP-expressing *E. coli in vivo* using real-time arresting by KCs (Fig. 6D). Digital quantification of phagocytosis efficiency revealed that KCs from mice fed HFD for 2 weeks displayed a slight increase in the arresting ability at initial time points after bacterial challenge with a concomitant reduction in bacterial counts in blood, which may explain the increased bacterial counts in the liver. In sharp contrast, mice fed HFD for longer periods had reduced ability to capture bacteria under flow, as shown by a significantly reduced frequency of KCs that ingested *E. coli* (Fig. 6E). We also tracked individual *E. coli* paths within sinusoids in order to estimate how fast bacteria were arrested upon entering the liver microcirculation (supplementary movies 3 and 4). Interestingly, we did not find differences in both track length and speed between the groups, indicating that despite the changes observed in KC number and arresting frequency, alternative mechanisms may operate to avoid free bacterial trafficking within sinusoids (Fig. 6F–H). Together, these data reveal 2 different scenarios that occur during the HFD ingestion protocol: i) an initial "priming" of KCs after 2 weeks on HFD that induced

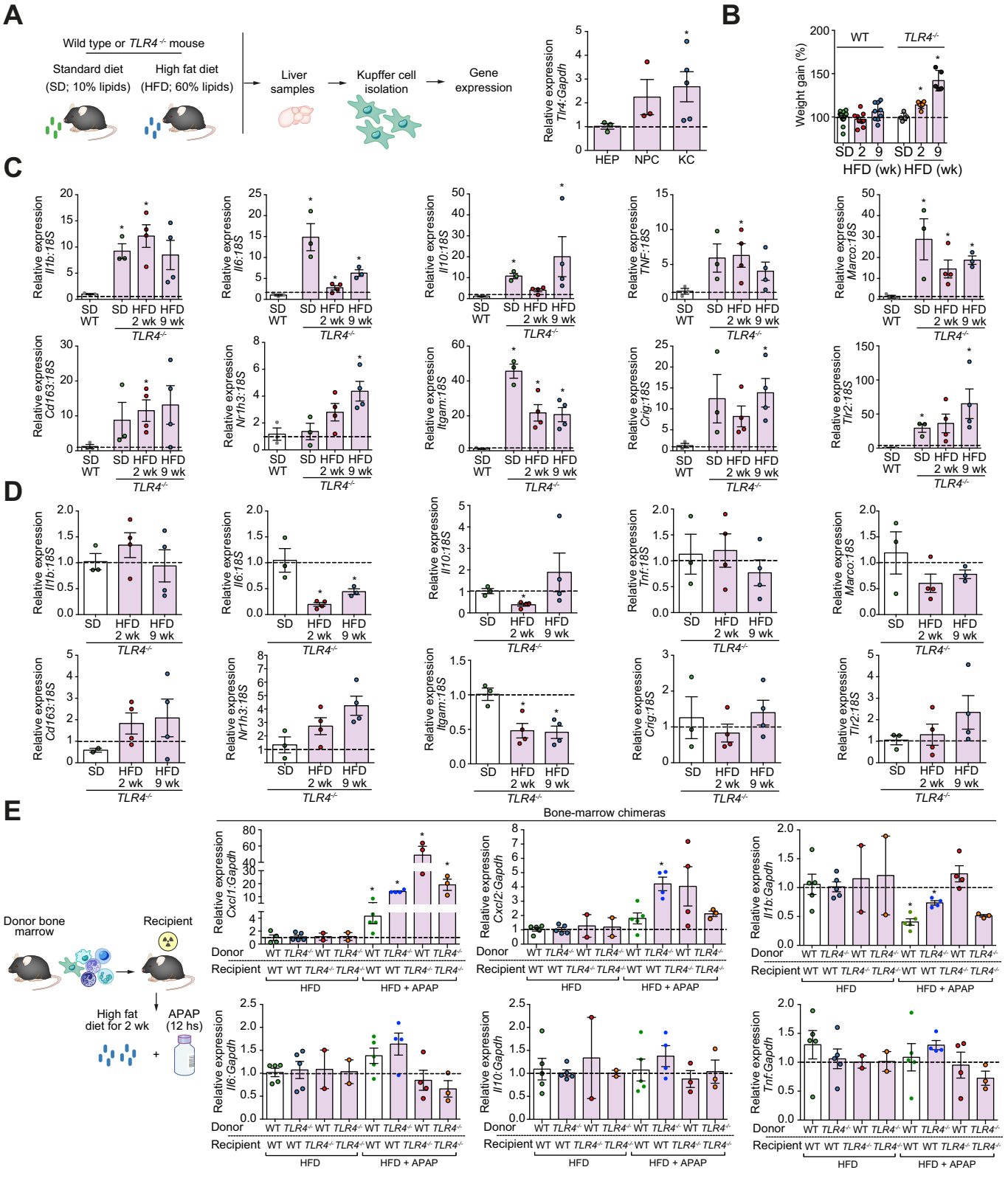

Fig. 8. Effects of TLR4 signaling in the early moments of NAFLD pathogenesis. (A) Expression of TLR4 in different liver compartments. (B) Mouse weight dynamics following HFD challenge using WT and *Tlr4*$^{-/-}$ mice. (C–D) Gene expression of different immune system pathways in isolated KCs. Mice (WT or *Tlr4*$^{-/-}$) were fed with SD or HFD (2 and 9 weeks) and fold change in gene expression was calculated compared to WT mouse fed SD (C). Cells were purified and gene expression was assessed by Real-Time PCR. (D) Same as (C), but fold change calculated compared to *Tlr4*$^{-/-}$ mice fed with SD. (E) Gene expression of different immune system pathways in liver samples collected from bone marrow chimeras. WT mice or *Tlr4*$^{-/-}$ mice were irradiated with gamma rays and endovenously received bone marrow hematopoietic precursors from WT or *Tlr4*$^{-/-}$ mice (WT >WT; WT >*Tlr4*$^{-/-}$; *Tlr4*$^{-/-}$ >*Tlr4*$^{-/-}$; *Tlr4*$^{-/-}$ >WT). After a recovery period (8 weeks

an increased ability to arrest bacteria, but with a reduced ability to kill engulfed *E. coli*; and ii) a dramatic change in KC biology from mice fed HFD for a period of 9 weeks, presenting not only a massive depletion, but also an inherent inability to arrest and kill bacteria by the remaining KCs.

Based on these major alterations on hepatic immune cells, and the relevance of macrophages to liver function, we next mapped immunologic alterations specifically in KCs isolated from mice fed HFD (Fig. 7). Interestingly, we found that the HFD induced a massive upregulation in several inflammatory and scavenger-related genes in KCs 2 weeks post challenge. Such changes were even more pronounced at later time points (9 weeks; Fig. 7). In agreement with samples from steatotic patients (Fig. 1B), we observed a large upregulation in *Tlr4* mRNA expression in KCs from HFD-fed mice, amongst other significant changes (Fig. 7). Taken together, these data demonstrate that the immunologic changes observed in liver NPCs, particularly a putative lost in KC tolerogenic profile, are an early consequence of short-term HFD ingestion.

Signaling via TLR4 drives KC tolerance in the initial phases of non-alcoholic fat liver disease

Emerging evidences indicate that chronic, low level elevation of gut-derived endotoxin may play a role in the establishment and progression of fatty liver disease, potentially driving liver inflammatory response via TLR4.[30,31] In fact, elevated endotoxin levels have been shown to be an aggravating factor for liver diseases. However, immunological tolerance triggered by the innate immune system has also been recognized as an anti-inflammatory mechanism that limits deleterious tissue injury in infections,[32] and TLR4 polymorphisms in humans may enhance complications during metabolic diseases.[33] Importantly, we found that *TLR4* gene expression was elevated in both humans and mice with NAFLD (Figs 1B, 4I and 7), suggesting that the TLR4 pathway either contributes to inflammation and consequently worsening of NAFLD or limits tissue injury induced by a HFD regimen. To investigate this dichotomic mechanism, we first fed WT mice and *Tlr4*$^{-/-}$ mice with both SD and HFD, evaluating their reaction to our dietary scheme (Fig. 8C, D) and the expression of different inflammatory pathways in KCs. Of note, TLR4 expression was detected in both hepatocytes and hepatic immune cells; however, TLR4 was expressed significantly more in KCs than in isolated hepatocytes (Fig. 8A), which led us to focus on KCs in the subsequent experiments. Gene expression analysis from isolated KCs revealed that deletion of TLR4 caused a massive upregulation in all genes evaluated, including *Il1b, Il6, Tnf* and *Il10*, even when SD was offered (Fig. 8C). Comparing the effects of the intake of SD or HFD by *Tlr4*$^{-/-}$ mice (Fig. 8D), we found profound differences in the expression of several inflammatory genes, suggesting that the absence of TLR4 altered the hepatic response to diet regardless of nutritional content (normal or high-fat load), impacting directly on body weight and KC gene expression (Fig. 8B–D). To dissect the specific contribution of TLR4 signaling in the different hepatic compartments, we lethally irradiated recipient WT and *Tlr4*$^{-/-}$ mice with gamma rays and engrafted bone marrow hematopoietic precursors from *Tlr4*$^{-/-}$ mice or WT controls (Fig. 8E). We have previously shown that almost 100% of immune cells that populated host livers after the recovering period were derived from donors using this irradiation/bone marrow transplant protocol.[28]

Comparing to controls fed with HFD for 2 weeks (WT >WT), we could not observe any significant changes in hepatic immune response in either WT mice that received bone marrow from *Tlr4*$^{-/-}$ mice or their WT counterparts (*Tlr4*$^{-/-}$ >WT). This led us to hypothesize that the HFD insult alone might not be enough to elicit putative alterations due to ablation of TLR4 signaling in different liver compartments. To induce a perturbation of higher magnitude within the liver environment, we decided to combine HFD insult with an APAP overdose, a well-established model of acute on chronic liver injury that has a major relevance to clinical practice. APAP intake alone (400 mg/kg; oral gavage) caused extensive centrilobular injury, with concomitant elevation of serum ALT and liver dysfunction (Fig. S4). Importantly, WT mice fed HFD for 2 weeks evolved to higher mortality rates, and increasing the HFD challenge period to 6 and 9 weeks in WT mice caused a dramatic increase in lethality due to APAP poisoning, reaching 100% mortality at 16 h (Fig. S4B). This revealed that APAP intoxication in combination with mild steatosis can led to a worse prognosis (Fig. S4). Interestingly, the complete absence of TLR4 (*Tlr4*$^{-/-}$ >*Tlr4*$^{-/-}$), absence in hepatic immune cells (*Tlr4*$^{-/-}$ >WT) or in hepatocytes (WT >*Tlr4*$^{-/-}$) led to a massive increase in the expression of neutrophil-related chemokines (*Cxcl1* and *Cxcl2*). Of note, substitution of embryonic KCs from bone marrow-derived macrophages (WT >WT) caused a significant reduction in *Il1b* expression during insult, which was not observed in other chimera groups (Fig. 8E). All other inflammatory pathways analyzed were not altered due to TLR4 absence, suggesting that chemokine production – either by macrophages or hepatocytes – might be strongly regulated by TLR4 signaling during hepatic inflammation, which could explain the massive neutrophil infiltration in the later phases of NAFLD. Thus, TLR4 signaling may potentially drive immune response tolerance and also metabolic control in the initial phases of NAFLD, because the absence of TLR4 promoted alterations in weight dynamics and enhanced expression of different inflammatory genes.

Discussion

Using novel approaches on high-end *in vivo* imaging procedures, combined with gene expression in different liver compartments, we demonstrated that the hepatic immune response is prematurely altered in the early phases of NAFLD development. This suggests that even in cases where only steatosis is observed, the hepatic immune response is already activated, deflecting the current concept that hepatic inflammation is a process that occurs in the late stages of NAFLD.[34,35] Both humans and mice displayed significant alterations in the expression of different inflammatory genes in the early development of NAFLD, a period in which a large percentage of individuals may be asymptomatic or present no laboratory alterations. In mice, even before any significant weight or metabolic alterations, ingestion of a diet

after irradiation), mice were fed with SD or HFD (2 weeks) and challenged with APAP (400 mg/kg, oral gavage). Samples were collected after 12 h of APAP challenge. Gene expression was assessed by Real-Time PCR. Fold change was calculated compared to chimera counterpart fed with an HFD. *p <0.05 compared to SD group (Student's t test). APAP, acetaminophen; HFD, high-fat diet; KCs, Kupffer cells; NAFLD, non-alcoholic fatty liver disease; SD, standard diet; TLR4, Toll-like receptor 4; WT, wild-type.

containing high levels of lipids led to enhanced inflammatory responses to drug injury, along with a relative inability to fight bacterial infections. Our data suggests that the hepatic immune system is the main sentinel for alterations in the liver lipid content, and despite initial suppression of immune responses, mice evolved to increase expression of almost all inflammatory genes evaluated in this study during the late phase of the dietary scheme. Hence, even during mild clinical manifestations, individuals with NAFLD might mount an inadequate hepatic immune response, which may account not only for enhanced chances of liver failure, but also for a reduced ability to clear blood-borne bacteria. In fact, KCs from HFD-fed mice displayed a reduced ability to engulf and kill blood-borne bacteria, which could be a consequence of the profound changes in the hepatic inflammatory milieu during the initial phases of NAFLD that can modify the KC immune profile. This may explain, in part, why patients with liver diseases frequently progress to sepsis and septic shock,[27,36] highlighting the pivotal role of the liver immune system in systemic defense.[26,37]

The liver has one of the most complex immune environments in the body, harboring several different subtypes of leukocytes even under homeostasis.[38] However, these populations can rapidly change their frequency and phenotype upon stimuli.[17,28] Herein, we have shown that the hepatic immune milieu is dramatically changed during early stages of NAFLD. In fact, liver leukocytes displayed a complex dynamic during the establishment of steatosis, because we found a massive depletion of DCs and KCs, along with disturbances in KC morphology and functionality. Fluctuations in DC frequency may be attributed to a possible experimental inaccuracy during differential DC x KC immunophenotyping, particularly upon inflammatory responses. In fact, a reliable gating strategy to differentially assess KCs and liver DCs is still under debate.[20,21,28,39] Importantly, an overt infiltration of neutrophils occurred at later time points (9 weeks), which was previously described as a key factor for enhanced collateral liver damage upon insults,[14,23,24,40,41] suggesting that such early alterations in these subpopulations may constitute a hallmark in the evolution from simple steatosis to steatohepatitis. However, it is reasonable to hypothesize that such overt neutrophil infiltration during NAFLD onset might also function as a backup strategy for bacterial clearance and phagocytosis while KCs are relatively absent. Therefore, our data highlighted the existence of a fine-tuned equilibrium within hepatic immune compartments, and alterations in leukocyte frequencies and phenotypes triggered by hepatic lipid accumulation may be considered as a putative marker for the early/mild stages of NAFLD.

Due to the its location between the intestine and systemic circulation, the liver is exposed to relatively large amounts of intestinally derived pathogen-associated molecular patterns in both healthy and disease states.[42] In this context, it is well accepted that under pathologic conditions, TLRs activate inflammatory signaling pathways in the liver and are actively involved in the pathophysiology of many hepatic diseases. However, TLRs may also play important roles in liver physiology by negatively regulating TLR-induced cellular responses.[30–32] Our data from both human and mouse samples revealed a biphasic behavior of immune response-related genes, displaying an initial suppression of several genes, along with upregulation of TLR4 expression during early steatosis. Even though this might be interpreted as a marker of immune system activation, it was interesting to observe that mice lacking TLR4 had several alterations in response to our dietary insult. *Tlr4*$^{-/-}$ mice gained significantly more weight upon HFD compared to WT controls, and we even observed disturbances in the expression of different genes involved in the immune response on the SD protocol. In fact, KCs lacking TLR4 naturally presented a pro-inflammatory phenotype even under regular dietary protocols. Also, when we replaced liver cells in WT mice with *Tlr4* knockout cells, the hepatic immune response to insults was completely altered. Of particular interest, chemokines involved in neutrophil recruitment and activation within the liver, which potentially increase hepatocellular damage during inflammation, were significantly upregulated in mice lacking TLR4 in immune cells or in hepatocytes, but not in controls. This suggests that signaling via TLR4 in liver cells may have opposite fates depending on the duration of the insult, acting as regulatory pathways in the initial phases of steatosis, and later as pro-inflammatory signals if the nutritional challenge persists. Also, significant alterations in the expression of chemokines in mice lacking TLR4 in hepatocytes suggest that TLR4 signaling is not only relevant in the immune system compartment, but also in liver parenchymal cells. This suggests that immune and metabolic systems within the liver may communicate to achieve a full organ response using TLR4 signaling, and alterations in this crosstalk may be not only a key trigger to organ dysfunction, but also for tissue homeostasis and tolerance.

In conclusion, we have shown that minor alterations in liver lipid content induced by short-term HFD are sufficient to rewire the liver immune response, triggering enhanced susceptibility to organ damage and infection upon insults. Thus, our data highlight that NAFLD diagnosis may be significantly improved by a more profound investigation focused on early changes in hepatic immunology. This may also guide customized nutritional and therapeutic interventions in patients at different stages of the NAFLD spectrum.

Abbreviations

ALT, alanine aminotransferase; APAP, acetaminophen; CFUs, colony forming units; DCs, dendritic cells; *E. coli*, *Escherichia coli*; HFD, high-fat diet; ITT, insulin tolerance test; KCs, Kupffer cells; NAFLD, non-alcoholic fatty liver disease; NAS, NAFLD activity score; NPCs, non-parenchymal cells; SD, standard diet; TLR4, Toll-like receptor 4; WT, wild-type.

Financial support

This work was supported by FAPEMIG, CAPES and CNPq (Brazil).

Conflict of interest

The authors declare no conflicts of interest that pertain to this work.

Please refer to the accompanying ICMJE disclosure forms for further details.

Authors' contributions

A.B.D., M.M.A. and B.A.D. performed confocal microscopy experiments and imaging analysis. C.X.L., J.A.S.G.E., T.C.M.F.C., B.R.S., C.A.C., L.C.F. and P.V.T.V. provided liver biopsies from humans. A.B.D., V.A.S.L., M.M.A., R.C.G., and D.M.A. performed non-parechymal cell flow cytometry experiment and analyzed data. A.B.D., E.C. and M.E.L performed bacterial infections experiments and analyzed data. A.B.D., A.M.A. and K.M.B. performed qPCR experiments and analysis. A.G.O. performed bioinformatics analysis of gene expression. A.B.D., M.M.A., B.N.L.N., M.A.F.L.,

D.M.A., S.C.M., B.A.D., M.M.S., H.M.C.O., C.D.M.M., K.M.O.C. performed *in vivo* experiments and analyzed data. A.B.D., M.M.A., V.A.S.L., R.C.G., D.M.A., M.S.M. and B.A.D. performed liver cells isolation and gene expression analysis. A.B.D., D.R.L., A.V.M.F., M.M.A. and V.A.S.L. performed biochemical analyses, oral glucose tolerance test and insulin tolerance test. S.R. and M.R. provided the diets and scientific input on diet development and protocol. G.B.M. designed the study. G.B.M. and R.M.R. wrote the paper.

Acknowledgements

We thank Dr Ricardo Gazzinelli (INCT-Vacinas), Dr. Mauro Martins Teixeira (INCT-Dengue), Nikon, Biolab Brasil, BD Biosciences for technical and financial support.

Supplementary data

Supplementary data to this article can be found online at https://doi.org/10.1016/j.jhepr.2020.100117.

References

[1] Chalasani N, Younossi Z, Lavine JE, Charlton M, Cusi K, Rinella M, et al. The diagnosis and management of nonalcoholic fatty liver disease: practice guidance from the American Association for the Study of Liver Diseases. Hepatology 2018;67:328–357.
[2] Younossi ZM, Koenig AB, Abdelatif D, Fazel Y, Henry L, Wymer M. Global epidemiology of nonalcoholic fatty liver disease-meta-analytic assessment of prevalence, incidence, and outcomes. Hepatology 2016;64:73–84.
[3] Estes C, Razavi H, Loomba R, Younossi Z, Sanyal AJ. Modeling the epidemic of nonalcoholic fatty liver disease demonstrates an exponential increase in burden of disease. Hepatology 2018;67:123–133.
[4] Younossi ZM, Blissett D, Blissett R, Henry L, Stepanova M, Younossi Y, et al. The economic and clinical burden of nonalcoholic fatty liver disease in the United States and Europe. Hepatology 2016;64:1577–1586.
[5] Estes C, Anstee QM, Arias-Loste MT, Bantel H, Bellentani S, Caballeria J, et al. Modeling NAFLD disease burden in China, France, Germany, Italy, Japan, Spain, United Kingdom, and United States for the period 2016-2030. J Hepatol 2018;69:896–904.
[6] Almeda-Valdes P, Cuevas-Ramos D, Aguilar-Salinas CA. Metabolic syndrome and non-alcoholic fatty liver disease. Ann Hepatol 2009;8(Suppl 1):S18–S24.
[7] Younossi ZM, McCullough AJ. Metabolic syndrome, non-alcoholic fatty liver disease and hepatitis C virus: impact on disease progression and treatment response. Liver Int 2009;29(Suppl 2):3–12.
[8] Singh S, Allen AM, Wang Z, Prokop LJ, Murad MH, Loomba R. Fibrosis progression in nonalcoholic fatty liver vs nonalcoholic steatohepatitis: a systematic review and meta-analysis of paired-biopsy studies. Clin Gastroenterol Hepatol 2015;13:643–654.e9. quiz e639–640.
[9] Friedman SL, Neuschwander-Tetri BA, Rinella M, Sanyal AJ. Mechanisms of NAFLD development and therapeutic strategies. Nat Med 2018;24:908–922.
[10] Younossi Z, Anstee QM, Marietti M, Hardy T, Henry L, Eslam M, et al. Global burden of NAFLD and NASH: trends, predictions, risk factors and prevention. Nat Rev Gastroenterol Hepatol 2018;15:11–20.
[11] Lynch CM, Kinzenbaw DA, Chen X, Zhan S, Mezzetti E, Filosa J, et al. Nox2-derived superoxide contributes to cerebral vascular dysfunction in diet-induced obesity. Stroke 2013;44:3195–3201.
[12] Santhekadur PK, Kumar DP, Sanyal AJ. Preclinical models of non-alcoholic fatty liver disease. J Hepatol 2018;68:230–237.
[13] Tsuchida T, Lee YA, Fujiwara N, Ybanez M, Allen B, Martins S, et al. A simple diet- and chemical-induced murine NASH model with rapid progression of steatohepatitis, fibrosis and liver cancer. J Hepatol 2018;69:385–395.
[14] Antunes MM, Araujo AM, Diniz AB, Pereira RVS, Alvarenga DM, David BA, et al. IL-33 signalling in liver immune cells enhances drug-induced liver injury and inflammation. Inflamm Res 2018;67:77–88.
[15] Nagy C, Einwallner E. Study of in vivo glucose metabolism in high-fat diet-fed mice using oral glucose tolerance test (OGTT) and insulin tolerance test (ITT). J Vis Exp 2018;(131):56672.
[16] Lacerda DR, Costa KA, Silveira ALM, Rodrigues DF, Silva AN, Sabino JL, et al. Role of adipose tissue inflammation in fat pad loss induced by fasting in lean and mildly obese mice. J Nutr Biochem 2019;72:108208.
[17] Nakagaki BN, Mafra K, de Carvalho E, Lopes ME, Carvalho-Gontijo R, de Castro-Oliveira HM, et al. Immune and metabolic shifts during neonatal development reprogram liver identity and function. J Hepatol 2018;69:1294–1307.
[18] Mehlem A, Hagberg CE, Muhl L, Eriksson U, Falkevall A. Imaging of neutral lipids by oil red O for analyzing the metabolic status in health and disease. Nat Protoc 2013;8:1149–1154.
[19] Marques PE, Antunes MM, David BA, Pereira RV, Teixeira MM, Menezes GB. Imaging liver biology in vivo using conventional confocal microscopy. Nat Protoc 2015;10:258–268.
[20] Liu Z, Gu Y, Chakarov S, Bleriot C, Kwok I, Chen X, et al. Fate mapping via Ms4a3-expression history traces monocyte-derived cells. Cell 2019;178:1509–1525.e19.
[21] David BA, Rubino S, Moreira TG, Freitas-Lopes MA, Araujo AM, Paul NE, et al. Isolation and high-dimensional phenotyping of gastrointestinal immune cells. Immunology 2017;151:56–70.
[22] Fonseca RC, Bassi GS, Brito CC, Rosa LB, David BA, Araújo AM, et al. Vagus nerve regulates the phagocytic and secretory activity of resident macrophages in the liver. Brain Behav Immun 2019;81:444–454.
[23] Marques PE, Amaral SS, Pires DA, Nogueira LL, Soriani FM, Lima BH, et al. Chemokines and mitochondrial products activate neutrophils to amplify organ injury during mouse acute liver failure. Hepatology 2012;56:1971–1982.
[24] Marques PE, Oliveira AG, Pereira RV, David BA, Gomides LF, Saraiva AM, et al. Hepatic DNA deposition drives drug-induced liver injury and inflammation in mice. Hepatology 2015;61:348–360.
[25] Kleiner DE, Brunt EM, Van Natta M, Behling C, Contos MJ, Cummings OW, et al. Design and validation of a histological scoring system for nonalcoholic fatty liver disease. Hepatology 2005;41:1313–1321.
[26] Jenne CN, Kubes P. Immune surveillance by the liver. Nat Immunol 2013;14:996–1006.
[27] Yan J, Li S, Li S. The role of the liver in sepsis. Int Rev Immunol 2014;33:498–510.
[28] David BA, Rezende RM, Antunes MM, Santos MM, Freitas Lopes MA, Diniz AB, et al. Combination of Mass cytometry and imaging analysis reveals origin, location, and functional repopulation of liver myeloid cells in mice. Gastroenterology 2016;151:1176–1191.
[29] Zeng Z, Surewaard BG, Wong CH, Geoghegan JA, Jenne CN, Kubes P. CRIg functions as a macrophage pattern recognition receptor to directly bind and capture blood-borne gram-positive bacteria. Cell Host Microbe 2016;20:99–106.
[30] Mencin A, Kluwe J, Schwabe RF. Toll-like receptors as targets in chronic liver diseases. Gut 2009;58:704–720.
[31] Schwabe RF, Seki E, Brenner DA. Toll-like receptor signaling in the liver. Gastroenterology 2006;130:1886–1900.
[32] Heymann F, Peusquens J, Ludwig-Portugall I, Kohlhepp M, Ergen C, Niemietz P, et al. Liver inflammation abrogates immunological tolerance induced by Kupffer cells. Hepatology 2015;62:279–291.
[33] Balistreri CR, Bonfigli AR, Boemi M, Olivieri F, Ceriello A, Genovese S, et al. Evidences of +896 A/G TLR4 polymorphism as an indicative of prevalence of complications in T2DM patients. Mediators Inflamm 2014;2014:973139.
[34] Nassir F, Rector RS, Hammoud GM, Ibdah JA. Pathogenesis and prevention of hepatic steatosis. Gastroenterol Hepatol (N Y) 2015;11:167–175.
[35] Yeh MM, Brunt EM. Pathological features of fatty liver disease. Gastroenterology 2014;147:754–764.
[36] Nesseler N, Launey Y, Aninat C, White J, Corlu A, Pieper K, et al. Liver dysfunction is associated with long-term mortality in septic shock. Am J Respir Crit Care Med 2016;193:335–337.
[37] Kubes P, Jenne C. Immune responses in the liver. Annu Rev Immunol 2018;36:247–277.
[38] Kubes P, Mehal WZ. Sterile inflammation in the liver. Gastroenterology 2012;143:1158–1172.
[39] Sierro F, Evrard M, Rizzetto S, Melino M, Mitchell AJ, Florido M, et al. A liver capsular network of monocyte-derived macrophages restricts hepatic dissemination of intraperitoneal bacteria by neutrophil recruitment. Immunity 2017;47:374–388.e6.
[40] Alvarenga DM, Mattos MS, Lopes ME, Marchesi SC, Araujo AM, Nakagaki BN, et al. Paradoxical role of matrix metalloproteinases in liver injury and regeneration after sterile acute hepatic failure. Cells 2018;7:247.
[41] Huebener P, Pradere JP, Hernandez C, Gwak GY, Caviglia JM, Mu X, et al. The HMGB1/RAGE axis triggers neutrophil-mediated injury amplification following necrosis. J Clin Invest 2015;125:539–550.
[42] Balmer ML, Slack E, de Gottardi A, Lawson MA, Hapfelmeier S, Miele L, et al. The liver may act as a firewall mediating mutualism between the host and its gut commensal microbiota. Sci Transl Med 2014;6:237ra266.